

THE SMALL SCALE ENVIRONMENT OF LOW SURFACE
BRIGHTNESS DISK GALAXIES

Gregory D. Bothun
Department of Physics
University of Oregon
Eugene OR 97403

James M. Schombert
IPAC/JPL
Cal. Inst. of Technology
Pasadena CA 91125

Christopher D. Impey and David Sprayberry
Steward Observatory
University of Arizona
Tucson AZ 85721
and

Stacy S. McGaugh
Department of Astronomy
University of Michigan
Ann Arbor MI 48109

ABSTRACT

We **usc** a sample of ≈ 340 low surface brightness (LSB) disk galaxies with measured redshifts in combination with the Center for Astrophysics redshift survey to test the hypothesis that LSB galaxies have a deficit of nearby companion galaxies compared to high surface brightness (HSB) disk galaxies. We find a very strong statistical deficit of galaxies located within a projected radius of 0.5 Mpc and within a velocity of 500 km s^{-1} around LSB disks compared to HSB disks. Furthermore, comparing LSB and HSB disks which are located in the same portion of the sky indicates that the average distance to the nearest neighbor is 1.7 times farther for LSB disks. A KS test rules out, at greater than the 99% confidence level, the hypothesis that the distribution of nearest neighbor distances is the same for HSB and LSB disks. We speculate that LSB disks have relatively long formation timescales and therefore must form in relative isolation. In addition, the lack of tidal interactions over a Hubble time serves to suppress the overall star formation rate as no external trigger is available to help clump the gas. The observed low surface densities of H I in combination with the low probability of tidal interactions effectively prevents these disks from evolving very rapidly.

1. INTRODUCTION

The evolutionary processes which determine the surface brightnesses of galactic disks remain enigmatic. Over the last five years, sufficient data in a variety of wavelengths has been gathered (e.g., McGaugh 1992; Knežek 1992; Schombert *et al.* 1992; Peletier and Willner 1992;) to effectively dispel the once popular notion that the central surface brightnesses of disk galaxies are a constant (see Freeman 1970; van der Kruit 1987). Instead, central surface brightness ($B(0)$) spans a large continuum of values but the space density of galaxies as a function of $B(0)$ remains unknown due essentially to 50 years of selection effects associated with the cataloging of galaxies. An intensive effort to alleviate this selection effect has been pursued by Schombert *et al.* (1992) and Impey *et al.* (1992). That effort has now detected hundreds of new disk galaxies whose contrast with the night sky background is only a few percent. This new class of galaxies, named low surface brightness (LSB) galaxies, has properties which are quite distinct from those that define the Hubble sequence (see McGaugh 1992).

The role that environment plays in the evolution of galaxies also remains enigmatic. The present arrangement of galaxies into clusters, low density but large scale walls, or shells surrounding large scale voids means that a wide range of environments exists. The existence of the morphology-density relation (e.g. Dressler 1980; Postman and Geller 1984) and the Butcher-Oemler effect (Butcher and Oemler 1978; see also Bothun and Dressler 1986; Dressler and Gunn 1990; Lavery *et al.* 1992) are the two most obvious examples of environmental influences on galaxy evolution. The physics of this influence, as well as its duration and at which redshift it is most effective, however, is not at all clear from the

available data. For instance, the role of merging and galaxy evolution is now under intense scrutiny. Some extreme positions (e.g., Schweizer *et al.* 1990, Lavery *et al.* 1992, Carlberg and Chariot 1992) suggest a rather larger merging rate which has led to the general galaxy population. Others acknowledge that merging is occurring now but downplay its overall prominence (e.g., Mihos *et al.* 1992, Majewski *et al.* 1992, Zepf 1992). A balanced perspective is offered by Hernquist (1992).

Clearly, mergers or interactions between galaxies will have the greatest probability of occurring in a low velocity dispersion environment in which several galaxies are embedded. The frequency of occurrence of galaxies in this type of environment depends both upon the unknown details of galaxy formation and large scale structure formation (e.g., the exact shape of the power spectrum). For instance, excess power on large scales is conducive to delayed infall of galaxies, which may have formed in relative isolation, towards denser structures. Furthermore, if the mean surface brightness of a galaxy is related to the amplitude of the initial density perturbation from which it formed, then there may well be a difference in the spatial distribution of high and low surface brightness galaxies. In particular, at a given mass, high surface brightness (HSB) galaxies would form more rapidly, from higher density perturbations and might be more strongly clustered and thus experience more interactions over a Hubble time. LSB galaxies, on the other hand might be more weakly clustered and experience less interactions. To date, the clustering properties of LSB galaxies compared to HSB galaxies have been studied only on a scale of 5-10 Mpc (see Bothun *et al.* 1986; Thuan *et al.* 1987; Schneider *et al.* 1990) and little is known about the smaller scale clustering properties.

Recent observations by van der Hulst *et al.* (1992) and McGaugh (1992) vividly show that the surface densities of H I throughout LSB disks are at or below the threshold criterion for star formation established in Kennicutt 1989 (see also Impey and Bothun 1989). Without a mechanism to clump this gas, star formation is unlikely to proceed on a large scale in these disks and hence their evolutionary progress is temporarily static. Indeed, it is unlikely that the star formation rate in the past in these galaxies was ever very high since this would leave, as a trace, a HSB reel component of the stellar population. In general, such a component is not seen in LSB disks with the possible exception that some of these galaxies do contain a normal bulge. Hence, there must be some mechanism which is operative in HSB disks but missing in LSB disks to account for the difference in star formation rates averaged over a Hubble time.

A clue to this mechanism comes from the recent work of Zaritsky and Lorrimer (1992) who have searched for companion galaxies around the LSB sample of Impey *et al.* (1992) and found a significant deficit compared to a control sample. They speculate that the lack of tidal interactions in LSB disks acts to suppress star formation and to keep the systems relatively static. Such speculation does have some theoretical basis (see Lacey and Silk 1991) and indeed, the tendency for some giant LSB disks to be isolated has been emphasized previously by Bothun *et al.* (1990) and may provide a key to their formation/survival (see also Hoffman, Wyse and Silk 1992). While better statistics are required to further progress in this area it has been our general impression, based on repeated visual inspection of images of LSB galaxies, that there is seldom another conspicuous galaxy nearby.

In this paper, we seek to quantify our visual impression by using redshift surveys to compare the clustering properties of LSB and HSB disk galaxies on a scale of 0-2 Mpc in order to statistically assess any differences, should they exist. Section 2 describes the LSB sample and the available control samples of HSB disks as well as our procedure for identifying companion galaxies. Section 3 presents the results of this comparison where it can be seen that the statistics strongly bear out our visual impression. Section 4 then discusses these results and suggests possible reasons why LSB galaxies inhabit sparser environments than HSB galaxies. All distances and scales are derived using $H_0 = 100 \text{ km s}^{-1} \text{ Mpc}^{-1}$.

2. Sample Characteristics and Reduction Technique

2.1 LSB Sample

Almost by definition, redshifts of LSB galaxies are difficult to obtain by optical means, unless they have a well-defined nucleus or bulge. Fortunately, however, many of these LSB disks are rich in H I and thus redshifts can be obtained at 21-cm. To date, the largest redshift surveys of LSB disk galaxies are those of Bothun *et al.* (1986), Schombert *et al.* (1992) and Impey *et al.* (1992). The survey of Bothun *et al.* (1986) comes exclusively from the UGC and the large scale clustering characteristics of that sample have been discussed by Bothun *et al.* (1986; see also Schneider *et al.* 1990). Most of those redshifts now appear in the redshift catalog maintained by the Center for Astrophysics (hereafter denoted ZCAT). Furthermore, owing to the relatively poor plate material, the UGC sample does not go to nearly as low of surface brightness levels as those of Schombert *et al.* (1992)

and Impey *et al.* (1992) (see discussion in Schombert and Bothun 1988). Hence, we form our LSB sample from the latter two recent surveys.

The Schombert *et al.* (1992) sample is derived from visual inspection of the plates of the Second Palomar Slcy Survey (POSS-II) and is confined to a narrow declination strip located at $20 \pm 10^\circ$. The spatial distribution of those galaxies with measured redshifts, together with the redshift distribution, is shown in Figure 1. The Impey *et al.* (1992) survey is a machine selected equatorial strip generated by APM analysis of UK Schmidt plates. Figure 2 displays the spatial and redshift distributions for that sample. The appearance of 'holes' in the spatial distribution for $\delta \leq 0$ is a reflection of the inability to obtain H I redshifts from Arecibo at those declinations. As Impey *et al.* (1992) discuss, the characteristics of this machine-selected sample are similar to the POSS-II sample. Both surveys have a similar depth and both surveys have similar redshift distributions, although the APM sample does have a larger percentage of galaxies with $v \geq 12,000$ km S⁻¹. Most of these higher velocity galaxies have had their redshifts determined from optical spectroscopy instead of at 21-cm.

2.2 HSB Comparison Sample

To form a comparison sample, we have searched through the electronic version of ZCAT as it was distributed in 1991 October. Several criterion are established to produce the desired end product, namely a sample of HSB disk galaxies with measured redshifts. To begin with, a magnitude and diameter must be tabulated, to compute a surface brightness which we parameterize as a surface magnitude defined as

$$sm = m_b + 5\log(D)$$

where D is the diameter measured in arcseconds. Magnitudes and diameters generally come from the Zwicky catalog, the UGC and the ESO catalog. Next we use the morphological information in *ZCAT* and only select objects which are tagged as having $T \geq 1$. Finally, since the relation between velocity and distance can become particularly contorted in the Local Supercluster, we restrict our analysis of both the HSB and LSB samples to objects with velocities $\geq 2000 \text{ km s}^{-1}$. This leads to a sample of 5704 disk galaxies. We now apply one additional velocity cut based on the empirical observation that few galaxies in the Zwicky, UGC or ESO catalogs have velocities $\geq 12,000 \text{ km s}^{-1}$. After applying this last criterion we are left with a sample of 5493 disk galaxies. The distribution of surface magnitudes for that sample is shown in Figure 3. It is remarkably Gaussian which is a likely manifestation of the selection effects first pointed out by Disney (1976) combined with large random errors in the tabulated magnitudes and diameters. To further obtain a sub-sample of HSB disk galaxies, we then select only those galaxies with mean surface brightness which is higher than the median shown in Figure 3. This leaves a sample of 2627 galaxies which have a mean surface brightness of $23.75 \pm 0.61 \text{ mag arcsec}^{-2}$. Curiously, this level of mean surface brightness is identical to the mean surface brightness of a Freeman disk (e.g., $\text{II}(O) = 21.65$) within the $B=25.0 \text{ mag arcsec}^{-2}$ isophote (equivalent to the mean surface brightness within ≈ 3 scale lengths). By comparison, the mean surface brightness within 3 scale lengths for the typical LSB galaxy in our sample is 1.5- 2.0 mag arcsec^{-2} less. In addition to this global sample of HSB spirals culled from *ZCAT*, we further divide it

into two subsamples which have the same sky coverage as the POSS-II and APM surveys. These two samples contain 870 and 137 galaxies respectively. The sparseness of the APM HSB sample renders it of little use as a comparison sample. We include it here only for the sake of completeness.

2.3 Finding Nearby Galaxies

Each individual HSB or LSB galaxy is then cross-referenced with the entire contents of *ZCAT* to search for other galaxies which are located within a certain velocity range and projected radius (in Mpc). These radius and velocity parameters are somewhat arbitrary but are uniformly applied to both samples. Here, we are not interested in applying any “friends-of-friends” algorithm for purposes of group identification as others (e.g., Ramella *et al.*) make that a specific focus of *ZCAT* analysis. Rather, we wish to roughly estimate the number of galaxies that are located in the same phase space element as an individual LSB or HSB galaxy. Based on properties of known groups, we searched in a cylinder of radius 2.4 Mpc and depth $\pm 500 \text{ km s}^{-1}$. Thus, for each LSB or HSB galaxy, we cycle through *ZCAT* and count the number of galaxies that are located within a projected radius of 2.4 Mpc and have a velocity within 500 km s^{-1} of that given galaxy. This yielded a sufficient number of ‘hits’ per galaxy that we are able to bin the radius parameter in units of 0.5 Mpc and to then compare the mean number of nearby galaxies in 4 radius intervals. In addition, we also record the actual distribution of projected separations for purposes of doing a nearest-neighbor analysis and to compare the cumulative distributions between the HSB and LSB samples using the KS test.

Care is taken to ensure that the search galaxy is not counted twice. In the case of HSB spirals this is easily done as the velocity of the search galaxy is identical to the listing in *ZCAT* (since it was culled from *ZCAT* in the first place). For the individual LSB galaxy, determining if it already has an entry in *ZCAT* is considerably more difficult for two reasons: 1) if it is in *ZCAT* then, in most cases, its velocity does not come from the H I detections of Schombert and Bothun (1988), Schombert *et al.* (1992) or Impey *et al.* (1992) and hence the velocity in *ZCAT* is not identical to that listed in those sources. Furthermore, there are small positional discrepancies between *ZCAT* and our master LSB catalog. Hence, we have assumed that any *ZCAT* hit which has a positional difference of $\leq 10''$ and a velocity difference of $\leq 100 \text{ km s}^{-1}$ is a real match to the search galaxy and does not represent another nearby galaxy. Approximately 10 % of the total LSD sample meet this criterion and inspection of the available image does not reveal another nearby galaxy. 2) a small number of galaxies selected to be LS13 arc, in fact, HSB galaxies which pronounced LSB extensions (see Schombert and Bothun 1988 for more detail). In general, these galaxies have very peculiar morphology and some seem to be of early type but have pronounced shell structure around them. The *ZCAT* entry for these galaxies can consist of 2 (or more) measurements as different knots of emission have been observed. A total of 8 LSB galaxies in the combined POSS + APM sample have been removed on this basis.

3.0 Search Results

3.1 Possible Biases

For our comparisons to be valid, we must ensure that there is no significant bias in either the redshift distribution or the sky coverage of *ZCAT* compared to the POSS-II and APM LSB surveys. For instance, if the median redshift of the LSB samples was significantly higher than that of *ZCAT*, this would lead to an artificial reduction in the number of ‘hits’ found in *ZCAT* for that LSB sample. Similarly, inadequate sky coverage in *ZCAT* in the LSB survey fields would also bias the comparison. The strip of sky corresponding to the POSS-II search (see Figure 1) contains 4482 entries in *ZCAT* in the velocity range 2,000–12,000 km s⁻¹ and covers $\approx 14\%$ of the sky. This yields a surface density of ≈ 0.8 *ZCAT* galaxies per square degree. The strip of sky corresponding to the APM search contains 1051 entries in *ZCAT* and corresponds to about 5% of the sky. This yields a surface density of ≈ 0.5 *ZCAT* galaxies per square degree. This reduced surface density is a reflection of the lower mean galactic latitude of the APM survey. Hence, the spatial distribution of the POSS-II LSB galaxies better matches the current sky coverage of *ZCAT*. We will take this factor into consideration in the subsequent analysis.

As discussed in § 2, we have restricted the velocity search range to $2000 \leq v \leq 12000$ km s⁻¹ for all samples. In the POSS search arm, the median redshift of the *ZCAT* sample is 6850 km s⁻¹ which, not surprisingly, is the approximate median redshift of the Great Wall (see Geller and Huchra 1989). For the LSB sample the median redshift is 5850 km s⁻¹. The median redshift of the *ZCAT* sample in the APM search area is 5750 km s⁻¹ which reflects the Perseus-Pisces Supercluster. The median redshift of the APM sample is 7200 km s⁻¹; significantly higher than *ZCAT* and hence incompleteness in the *ZCAT* sample will be more significant in this sample. This coupled with the reduced

surface density coverage of *ZCAT* in the APM search area indicates that the ensemble average of companion galaxies in the APM LSB sample will be artificially less than the POSS-II sample. This is indeed borne out in the analysis (see below) but we can partially compensate for this bias by using velocity filtering on the data.

3.2 Comparison of Mean Number of Companions

The simplest statistic which can be formulated just involves counting companions out to a specified radius (≈ 2.4 Mpc in this case). While this statistic carries virtually no spatial information, it does provide a rough test of the hypothesis that LSB galaxies have, on average, fewer nearby galaxies than HSB disk galaxies. Table 1 presents the results of these raw counts. In table 1, column 1 specifies the sample and column 2 gives the velocity range. Column 3 gives the projected radius out to which the counts were made while column 4 gives the number of galaxies used in formulating the sample mean (column 5). In general, mean quantities are calculated after one cycle of 2.5σ rejection. The number of rejected galaxies is given in parenthesis in column 4. The first 6 rows of Table 1 refer to all companions contained within a projected radius of 2.4 Mpc and the means are formed without any rejection. Error bars on these means represent root N counting noise. For the remaining entries in this table mean counts are given in annuli of width 0.5 Mpc. Error bars are σ/\sqrt{N} .

The basic result is that the combined APM + POSS LSB sample is deficient in companions at the 5.6σ level compared to HSB spirals in *ZCAT*. Note also, that since there are $\approx 36,000$ galaxies contained in *ZCAT*, 50% of them are located within a projected radius of 2.4 Mpc from some HSB spiral. The next level of analysis involves binning the

data by radius and velocity. To account for possible velocity bias and differential incompleteness effects in sample comparisons, we subdivide each HSB and LSB sample into two velocity regimes. The low velocity regime is defined by $2000 \leq V \leq 7000 \text{ km s}^{-1}$ and the high velocity regime is defined by $7000 \leq V \leq 12000 \text{ km s}^{-1}$. Table 2 summarizes the differences between the means, in units of σ , in the comparison of various LSB and HSB samples. The POSS and APM samples are compared at radii of 0.5, 1.0, 1.5 and 2.0 Mpc to the total HSB sample as well as to the respective HSB sample that covers the equivalent area of sky. As stated earlier, the APM HSB comparison sample will not yield significant results owing to its small size.

Figure 4 graphically summarizes the information contained in Table 2. The plotted error bars are $\pm 2\sigma$ in length. The statistically poor APM HSB sample is omitted from these Figures. A fuller discussion of these results is presented in the next section. We briefly note here that 1) in all velocity cuts and at all radius bins, there is a highly significant difference in the mean number of companion galaxies between the HSB and LSB samples, 2) the APM and POSS samples generally track each other very well, and 3) *ZCAT* exhibits a more clustered behavior in the POSS search region than over the whole sky. The differences are particularly significant at the high velocity end which means that the POSS search region has been more thoroughly covered by *ZCAT*.

3.3 Nearest Neighbor Distribution

Another statistical test for investigating differences in the small scale environment between HSB and LSB samples involves determining the mean projected distance to the closest galaxy. However, in addition to noting the mean difference we can also apply the

KS test on the respective cumulative distribution functions. This was done by binning the distance to the nearest projected galaxy in bins of width 0.2 Mpc from 0 to 2.4 Mpc. These results are summarized in Table 3 and graphically shown in Figure 5. In table 3, column 1. gives the sample, column 2 gives the number of galaxies which have at least 1 companion within a projected radius of 2.0 Mpc, column 3 gives the velocity range and column 4 gives the mean projected distance and its error to the nearest companion. Column 5 and 6 give the KS statistic D_{max} . The number in parenthesis is the confidence level that D_{max} exceeds. For very large samples, D_{max} asymptotically approaches a value of .163 at the 99% confidence interval. Clearly, the KS test strongly rejects the hypothesis that the distribution of nearest neighbor distances is the same for the HSB and LSB samples. Importantly, the KS test also shows that the nearest neighbor distributions for all the various HSB samples are consistent with one another and that the APM and POSS LSB samples are consistent with each other.

4 Discussion

4.1 A Lack of Nearby Companions

The statistical results presented in § 3 strongly show that there is a deficit of other galaxies around LSB galaxies as compared to HSB galaxies. This deficit appears to be quite real. We can not account for any selection effect which would result in such a pronounced difference. For instance, both the visual search of the POSS and the machine search of the APM were blind to the presence of other galaxies; that is, we did not look only where there were no other galaxies. Since the median redshifts of the various HSB and LSB samples are roughly similar, this deficiency of galaxies nearby to LSB samples is also not

the result of redshift incompleteness in *ZCAT*. Moreover, although the difference in mean number of companions is very significant between all the LSB and HSB samples, it is most pronounced between the POSS LS13 sample and the *ZCAT* HSB sample which is located in the POSS search area. We emphasize that this area of the sky has been the most heavily surveyed for inclusion in *ZCAT* and hence represents the fairest comparison, especially in the $2000 - 7000 \text{ km s}^{-1}$ velocity range.

From the data in Table 1 for the POSS LSB and HSB samples, we see that the deficit in the number of galaxies grows from 0.89 ± 0.05 at $r=0.5 \text{ Mpc}$ to 2.71 ± 0.40 at $r=2.0 \text{ Mpc}$. The best fit linear slope for the POSS HSB sample to the 4 data points plotted in Figure 4 is 3.08 ± 0.18 compared to 2.42 ± 0.24 for the LSB sample; a marginally significant (2.4σ) difference. Hence, normalized to the $r=0.5 \text{ Mpc}$ bin, the LSB sample would appear to contain a deficit of galaxies at larger radii in comparison to the HSB sample. However, to draw this conclusion from examining the data in this manner is quite erroneous since the $r=2.0 \text{ Mpc}$ data point represents 16 times more projected area. Therefore, the relevant quantity to plot is surface density of galaxies. This is shown in Figure 6, where the surface density now includes the search galaxy itself. This Figure makes it quite clear that, in all velocity intervals, the deficit between HSB and LSB galaxies occurs primarily at small radii. At progressively larger radii, the surface density around LSB galaxies smoothly merges with that around HSB galaxies, although the apparently small differences at $r=2.0 \text{ Mpc}$ remain significant.

This behavior is consistent with the results of the nearest neighbor analysis shown in Figure 5, where the largest difference also occurs at the smaller radii. It is also consistent

with the assertions of Schombert *et al.* (1992), Thuan *et al.* (1987) and Bothun *et al.* (1986) that, on scales ≥ 5 Mpc, there is no difference in the spatial distribution of HSB and LSB galaxies. Hence, the principle difference between the small scale environments of HSB and LSB galaxies is that LSB galaxies tend to have significantly fewer galaxies in their immediate vicinity. This result is also highly consistent with the visual search results of Zaritsky and Lorrimer (1992), conducted for the APM sample. Comparing the POSS HSB and LSB samples indicates that, on average, the nearest neighbor to a LSB disk galaxy is located 1.7 times farther than the typical separation between a HSB galaxy and its nearest neighbor. Interestingly, there is also a difference in the mean velocity separation of companions between the POSS HSB and LSB samples. In particular, the 6740 galaxies found around the POSS HSB spirals have a mean velocity difference of $-10 \pm 3 \text{ km s}^{-1}$. An ensemble average of zero would be expected in the case where all HSB spirals are members of bound groups or clusters. Conversely, the 625 companions found around the POSS LSB spirals exhibit a significant peculiar velocity of $207 \pm 6 \text{ km s}^{-1}$, which indirectly suggests that most LSB disks are not, on average, at rest with respect to nearby galaxies and hence are not members of bound groups.

4.2 LSB Galaxies in Diverse Environments

The results discussed above show that, on average, LSB disk galaxies lack nearby companions. But, does this imply that all LSBs are situated in locally sparse environments? Figure 7 shows the distribution of the number of companions within $r = 0.5$ and $r = 2.0$ Mpc for the combined APM and POSS LSB sample within the $2\text{-}7000 \text{ km s}^{-1}$ velocity range. This Figure demonstrates that, while LSB isolation on a scale of 0.5 Mpc is common,

it is rare on a scale of 2.0 Mpc as 80 % of the sample have at least one other galaxy located within that radius. Moreover, ≈ 20 % of the sample are located in populous environments of 8 galaxies or more. Tables 4 and 5 list the 38 most isolated LSBs and the 37 most populous LSBs. A populous LSB is defined as one having either 3 or more companions within a projected radius of 0.5 Mpc or 8 or more companions with a projected radius of 2.0 Mpc. An isolated LSB is one defined as having zero companions in *ZCAT* out to a projected radius of 2.0 Mpc. Of course, there could be nearby projected galaxies that are not in *ZCAT* and therefore we performed a visual inspection of the plate material for all the galaxies listed in Table 4. The results of that inspection are listed in the comments column. In most cases, this visual inspection also revealed the galaxy to be isolated. In a few cases, small galaxies were located nearby but these all appear to be background based on their HSB and small angular size. However, two galaxies (F893-11 and F683-1) definitely appear to be associated with companions whose redshifts are not (yet) in *ZCAT*. For the populous LSB galaxies, either the name of the brightest galaxy within 2.0 Mpc or that of a known structure near the galaxy is listed in Table 5.

The mean redshift of the isolated LSBs 3975 ± 520 km s⁻¹ while that of the popular LSBs is 3084 ± 480 km s⁻¹; no significant difference. The distribution on the plane of the sky of the isolated and populous LSBs is shown in Figure 8 in velocity strips 1000 km s⁻¹ wide. Most of the populous LSBs are associated with known large scale structures such as the Cancer or Pegasus, or are located near groups associated with the Perseus-Pisces Supercluster, Coma-A1367 structure, or the A 194- A400 complex. Figure 9 shows the spatial distribution around the populous LSBs listed in Table 5. For those in clusters

(e.g., the F495 or F677 objects) only one example is shown. In general, the LSB sits on the edge of the distribution and only in a few cases (e.g., F544-1 in the NGC 772 group) does it appear to be a real member of a group. In most cases, although there are a large number of galaxies located within a projected radius of 2.0 Mpc, the LSB remains isolated on a scale of 0.5 Mpc. In some cases, (e.g., F61 1-1) the LSB is a true dwarf irregular galaxy which is a member of a small group. The distribution of the most isolated LSB galaxies in the lowest three velocity slices is somewhat sporadic with only a loose association with known structures. However, in the highest two velocity slices there is a clear clustering of objects with $150 \leq \text{ra} \leq 200$ and declination $\approx 20^\circ$. This clustering is particularly apparent in the highest velocity slice. The dominant structures in this part of the sky are the Coma Supercluster (at mean redshift $\approx 7000 \text{ km s}^{-1}$) as well as the Great Wall. Most of the isolated LSBs are part of the Great Wall structure, once again, indicating that they are reliable tracers of structure on large scales. Most importantly, however, is that we can discern no difference in the overall morphology or mean surface brightness between the isolated and populous LSBs. Hence, if environment and surface brightness are linked, then it would appear to be the small scale environment (e.g., $r \leq 0.5 \text{ Mpc}$) which is the most important.

4.3 Possible Reasons for LSB Isolation

In this subsection we consider possible reasons behind the observed paucity of other galaxies within 0.5 Mpc and within 500 km s^{-1} of our sample of LSB disk galaxies. Two basic options spring to mind. The first appeals to some intrinsic formation scenario while the second involves the effects of a limited number (or none) of tidal interactions over

a Hubble time. Although the mass-to-light ratios of LSB disk galaxies are still not well known, the available data is consistent with the idea that, at a given mass, LSB galaxies represent lower initial density fluctuations. For any Gaussian filtering of a CDM power spectrum, lower density fluctuations correspond to lower σ and hence more common fluctuations. For instance, at a mass scale of $10^{10} M_{\odot}$, a typical LSB disk forms from a 0.5σ fluctuation whereas a typical HSB disk forms from a 2.5σ fluctuation (see McGaugh *et al.* 1993 for more details). The key to successful galaxy formation, however, is that a fluctuation is isolated and therefore allowed to collapse free from external perturbations. Most low σ peaks are located on the "shoulders" of higher σ peaks and hence will quickly merge into the formation of a single, denser object. Unfortunately, current N-body simulations lack the resolution to determine the statistics of isolated peaks on a scale of 1 Mpc, but we note here that potentially, the existence of these isolated LSB galaxies can help constrain such higher resolution simulations.

In this sense, the existence of isolated LSBs is not a confirmation of biased galaxy formation because the scales are much too small. Biasing, in the context of current generation N body simulations, suggests that objects which formed from $\approx 1\sigma$ peaks should be less clustered on large scales (5-10 Mpc) than objects which formed from the much more rare 3σ peaks. Those simulations, however, can not be easily extrapolated to smaller scales to predict that, on a size scale of 1 Mpc, lower σ peaks would preferentially be devoid of nearby objects which formed from higher σ peaks (e. g., HSB galaxies). Furthermore, as demonstrated above, the overall surface density environment of LSB galaxies, on a scale size of 2.0 Mpc, is not very different than that, of HSB spirals. Since there is unlikely to

be any physical difference between the formation of structure on 2.0 and 0.5 Mpc scales, it seems quite improbable that isolated LSB galaxies result from some fundamentally different manner of the collapse of initial density perturbations.

A more likely scenario, in the context of galaxy formation, appeals to an extension of the argument for the existence of the morphology density relation (e.g., Dressier 1980; Postman and Geller 1984). Here it is suspected that the longer formation timescales of disks, relative to spheroids, makes it quite difficult for a disk to form in a high density environment. Since a lower initial density contrast naturally leads to longer formation (collapse) time then LSB disks are particularly prone to being destroyed in dense environments (though remember, they are found in loose clusters such as Cancer and Pegasus). Hence, it seems likely that these objects did initially form in relative isolation and like other galaxies, have since migrated to inhabit larger scale structures. This scenario then suggests that, since LSB galaxies are observed to have the same large scale clustering properties as the rest of the galaxy population, they were more weakly clustered at higher redshift. Hence, they may be related to the weakly clustered population of faint, blue galaxies observed by Lilly *et al.* (1991) although we stress that our sample of LSB objects are unlikely to be the faded remnants of a higher redshift population (see Babul and Rees 1992) because they are still quite blue,

Finally, we consider the obvious. Our sample of LSB galaxies tends to avoid the group environment. It is this low velocity dispersion environment which is most conducive for strong tidal interactions. Although LSBS are also found in clusters, that environment is

not conducive to interactions due to the high relative velocities of the potential participant galaxies. The lack of tidal disturbances over a Hubble time may have two important effects on the evolution of LSB disks. Mihos *et al.* (1991) have studied the effects of an interaction on both the stellar and gaseous distributions in disk galaxies. They find that most interactions result in an increase in the star formation rate as the gas is perturbed and becomes more clumped. McGaugh *et al.* (1993) and van der Hulst *et al.* (1992) show that, in general, the H I surface density in LSB disks is below the suspected threshold for star formation to occur. In addition, LSB disks appear to be highly deficient in molecular material (Schombert *et al.* 1990; Knezek 1992). Hence, without an external agent to disrupt the gas distribution, these LSB galaxies will continue to evolve slowly as the time averaged star formation rate remains low. A similar conclusion has been reached by Zaritsky and Lorrimer (1992). Our LSB sample also contains no examples of inner bars, a feature that usually does arise in a tidal encounter and which can dynamically channel gas into higher density regions thus facilitating star formation.

In addition to perturbing the star formation rate, tidal interactions also cause mass to be lost from galaxies. Hence, isolation from tidal interactions aids the survivability of systems with low surface mass density and hence low gravitational restoring force. This seems especially critical in the case of the very large LSB disks such as Malin 1 whose scale lengths are typically larger than 10 kpc. Indeed, most of these very large objects are quite isolated (see Knezek 1992). However, we emphasize here that, on average, our sample galaxies have only a factor of 4 less surface mass density (assuming similar M/L as HSB spirals). If anything, the M/L for LSB galaxies is likely to be higher which would reduce the surface

mass density discrepancy. In a purely exponential mass distribution, the $1/2$ mass radius occurs at 1.7 scale lengths, which corresponds to a surface brightness of $23.5 \text{ mag arcsec}^{-2}$ for a Freeman disk. Tidal damage can be expected to occur mostly at radii beyond the $1/2$ mass point and this is borne out both in simulations and observations of real interacting galaxies (see Mihos 1992). Since the typical central surface brightness of our sample LSB galaxies is $23.0 \text{ mag arcsec}^{-2}$, then most of our sample galaxies would easily survive a tidal encounter and would not be totally destroyed if located in the group environment. We thus believe that the lack of exposure to tidal interactions is more effective at suppressing the global star formation rate and the overall evolutionary timescale of the disk than it is in preserving these objects to be discovered at the present epoch.

5 Summary

We have used a sample of ≈ 340 LSD galaxies with measured redshifts to investigate their small scale clustering characteristics in comparison with samples of HSB spirals culled from the Center for Astrophysics redshift survey catalog. Care has been taken to minimize any possible bias due to incompleteness in redshift in either the HSB or LSB samples. In addition to a whole sky comparison sample of HSB spirals, we have formed subsamples which duplicate the sky coverage of the LSB samples. This is particularly important in the case of those LSB spirals selected from the FOS S-I I survey since that region of the sky shows the highest degree of clustering in *ZCAT*. To form our analysis we have searched through our master LSB catalog in combination with *ZCAT* to find all galaxies which are located within a projected radius of 2.0 Mpc and within a velocity of 500 km s^{-1} of

individual HSB and LSB spirals. Based on a comparison of the relative populations in this phase space we conclude the following:

1. There is a pronounced and highly significant, deficit of galaxies with projected separations less than 0.5 Mpc in the LSB sample. The mean projected distance to the nearest neighbor is ≈ 1.7 times farther for LSB than HSB spirals which are located in the same portion of the sky. A KS test rejects, at greater than the 99% confidence level, the hypothesis that the distribution of nearest neighbor distances is same for HSB and LSB spirals.

2. Although there remains a significant deficit of galaxies around LSB galaxies out to $r = 2.0$ Mpc, the respective surface densities of HSB and LSB galaxies being to merge at larger radii. This is consistent with earlier observations (Bothun *et al.* 1986, Thuan *et al.* 1987, Schneider *et al.* 1990, Schombert *et al.* 1992) that, on scales ≥ 5 Mpc, LSB galaxies trace out the same structures as HSB galaxies.

3. Although LSB disks have a pronounced deficit of nearby galaxies, not all LSBs are confined to that regime. In particular, several LSBs are found in 100SC clusters or on the periphery of groups. However, LSB disks are very rarely found inside groups. There appears to be no difference between the appearance or mean surface brightness of the most isolated LSBs compared to the ones which are found in or near the densest regions.

4. The data are consistent with the notion that LSB disk galaxies have experienced fewer tidal encounters, over a Hubble time, compared to HSB spirals. While the net effect of this on the physical evolution of these systems is not clear, we have argued that the lack of tidal interactions serves to suppress the overall star formation rate as an external

trigger to clump the H I is not available. Without such a tidal trigger, the low observed surface densities of H I in these systems renders their evolutionary rate rather slow. For galaxies with a normal IMF, the mean surface brightness is a direct reflection of the average star formation rate over a Hubble time. Hence, it may well be that the distinguishing characteristic between HSB and LSB disk galaxies is the net number of tidal interactions that each has experienced over a Hubble time.

5. If LSB disks are the result of initial density perturbations of relatively low amplitude, then their relative isolation on small scales has a natural explanation on two grounds: 1) For any Gaussian filtered power spectrum, most low density contrast, low σ peaks will not be isolated and hence are destined to merge early on with the rarer higher density perturbations which eventually make luminous galaxies. To avoid this merger, would require a low σ peak that is well isolated. 2) Low density contrast perturbations will have longer collapse times and hence are more prone to disruption in dense environments. Hence, the observation that many LSB disks are relatively isolated is an additional manifestation of the well established density-morphology relation, but is not, by itself, a manifestation of biased galaxy formation,

We close by emphasizing that there likely exists two distinct classes of LSB galaxies; only one of which has been discussed here. In particular, conclusion #5 is based on an unproven assumption, namely that the: M/L ratio of LSB and HSB disks are similar so that LSB directly reflects lower volume and surface mass density. It is, of course, possible that LSB is reflecting a dim, high hi/L stellar population, in which case the volume mass density is not necessarily any lower than it is for normal galaxies. Currently, it is virtually

impossible to obtain the necessary dynamical data for estimating M/L so this question is likely to linger for some time. If indeed some LSBS have high M/L then we might expect to find them in high density environments and indeed Impey *et al.* (1988) do find many examples in the Virgo cluster. These, however, are uniformly H I poor and devoid of any current star formation. In addition, their mean surface brightness is at least 1 mag arcsec^{-2} lower than the typical H I rich LSB disk contained in this sample and they are typically an order of magnitude lower in total luminosity. These cluster LSB dwarfs likely have a very different formation and evolutionary scenario than we have outlined for our sample of LSB disks.

We thank John Huchra and the CFA Redshift Team for continuing to provide an extremely valuable service to the astronomical community which helped to make this project feasible,

REFERENCES

- Babul, A., and Rees, M. 1992, *M. N. R. A. S.*, **255**, 346.
- Bothun, G., Beers, T., Mould, J. and Huchra, J. 1986, *Ap. J.*, **308**, 510.
- Bothun, G., Schombert, J., Impey, C., and Schneider, S. 1990, *Ap. J.*, **360**, 427.
- Butcher, H. and Oemler, A. 1978, *Ap. J.*, **219**, 18.
- Carlberg, R., and Chariot, P. 1992 preprint.
- Disney, M. 1976, *Nature*, **263**, 573.
- Dressler, A. 1980, *Ap. J.*, **236**, 351.
- Dressler, A. and Gunn, J. 1990, in *Evolution of the Universe of Galaxies: Edwin Hubble Centennial Symposium*, ed. R. Kron, (San Francisco: Astronomical Society of the Pacific), p. 200.
- Freeman, K. 1970, *Ap. J.*, **160**, 811.
- Geller, M. and Huchra, J. 1989, *Science*, **246**, S79.
- Hernquist, L. 1992 in *The Evolution of Galaxies and Their Environment: Third Teton Summer School* ed. H. Thronson and M. Shun, in press.
- Hoffman, Y., Wyse, R., and Silk, J. 1992, *Ap. J. Letters*, **388**, L13.
- Impey, C., Bothun, G., and Malin, D. 1988, *Ap. J.*, **330**, 634.
- Impey, C. and Bothun, G. 1989, *Ap. J.*, **341**, 89.
- Impey, C., Irwin, M., Sprayberry, D., and Bothun, G. 1992 preprint.
- Kennicutt, R. 1989, *Ap. J.*, **344**, 685.
- Knežek, P. 1992 Ph. D. Thesis, Univ. of Massachusetts.
- Lacey, C. and Silk, J. 1991, *Ap. J.*, **381**, 14.
- Lavery, R., Pierce, H., and McClure, R. 1992 *A. J.* in press.
- Lilly, S., Cowie, L. and Gardner, J. 1991, *Ap. J.*, **369**, 79.

- Majewski, S., Hereld, M., Koo, D., Illingworth, G. and Heckman, T. 1992 preprint.
- McGaugh, S. 1992 Ph. D. Thesis, Univ. of Michigan.
- McGaugh, S., Bothun, G., Schombert, J. and van der Hulst, T. 1992 preprint.
- Mihos, C., Richstone, D., and Bothun, G. 1991, *Ap.J.*, 377, 72.
- Mihos, C., Richstone, D., and Bothun, G. 1992 *Ap.J.* in press.
- Mihos, C. 1992 Ph. D. Thesis, Univ. of Michigan,
- Peletier, R. and Willner S. 1992, *A. J.*, 103, 1761.
- Postman, M., and Geller, M. 1984, *Ap.J.*, 281, 95.
- Schneider, S., Thuan, T., Magri, C. and Wadiak, J. 1990, *Ap.J. Supp.*, 72, 245.
- Schombert, J. and Bothun, G. 1988, *A. J.*, 95, 1392.
- Schombert, J., Bothun, G., Impey, C. and Mundy, L., *A. J.*, **100**, 1523.
- Schombert, J., Bothun, G., Schneider, S., and McGaugh, S. 1992, *A. J.*, **103**, **1107**.
- Schweizer, F., Seitzer, P., Faber, S., Burstein, D., Dalle Ore, C. and Gonzalez, J. 1990, *Ap. J. Letters*, 364, L33.
- Thuan, T., Gott, R., and Schneider, S. 1987, *Ap.J. Letters*, 315, L93.
- van der Kruit, P. 198x, *Astr. Ap.*, **173**, 59.
- van der Hulst, T., Skillman, E., Smith, T., Bothun, G. and McGaugh, S. 1992 preprint.
- Zaritsky, D. and Lorrimar, S. 1992 in *The Evolution of Galaxies and Their Environment: Third Teton Summer School* ed. H. Thronson and M. Shun, in press.
- Zepf, S. 1992 preprint.

Table 1. Summary of Counts

Sample	Vel. Range km/s	Rad Mpc	No. Gal.	Mean Counts Galaxies
ALL HSB	2-12000	2.4	2627	6.92 ± 0.20
POSS HSB	2-12000	2.4	870	7.74 ± 0.38
APM HSB	2-12000	2.4	137	6.39 ± 0.85
ALL LSB	2-12000	2.4	321	4.51 ± 0.38
POSS LSB	2-12000	2.4	135	4.63 ± 0.68
APM LSB	2-12000	2.4	186	4.42 ± 0.53
ALL HSB	2-12000	0.5	2558 (69)	0.76 ± 0.02
		1.0	2567 (60)	1.90 ± 0.05
		1.5	2551 (76)	3.21 ± 0.08
		2.0	2537 (90)	4.68 ± 0.11
	2-7000	0.5	1808 (50)	0.85 ± 0.03
		1.0	1809 (49)	2.19 ± 0.06
		1.5	1799 (59)	3.77 ± 0.10
		2.0	1785 (73)	5.56 ± 0.13
	7-12000	0.5	754 (15)	0.58 ± 0.04
		1.0	752 (17)	1.10 ± 0.07
		1.5	751 (18)	1.55 ± 0.11
		2.0	753 (16)	2.61 ± 0.15
POSS HSB	2-12000	0.5	851 (19)	1.02 ± 0.05
		1.0	848 (22)	2.14 ± 0.10
		1.5	845 (25)	3.59 ± 0.15
		2.0	845 (25)	5.23 ± 0.21
	2-7000	0.5	538 (10)	1.13 ± 0.06
		1.0	533 (15)	2.35 ± 0.12
		1.5	529 (19)	3.93 ± 0.18
		2.0	527 (21)	5.74 ± 0.24
	7-12000	0.5	312 (10)	0.80 ± 0.09
		1.0	313 (9)	1.71 ± 0.19
		1.5	313 (9)	2.82 ± 0.25
		2.0	312 (10)	3.87 ± 0.31
APM HSB	2-12000	0.5	131 (G)	0.47 ± 0.07
		1.0	134 (3)	1.57 ± 0.16
		1.5	131 (i)	2.50 ± 0.23
		2.0	131 (3)	3.76 ± 0.35
	2-7000	0.5	91 (3)	0.66 ± 0.11
		1.0	91 (3)	1.82 ± 0.20
		1.5	91 (3)	3.35 ± 0.38
		2.0	88 (G)	4.53 ± 0.45
	7-12000	0.5	30 (1)	0.07 ± 0.04
		1.0	30 (1)	0.60 ± 0.12
		1.5	30 (1)	0.93 ± 0.18
		2.0	30 (1)	1.10 ± 0.20

Table 1. Summary of Counts

Sample	Vel. Range km/s	R ad Mpc	No. Gal.	Mean Counts Galaxies
POSS LSB	2-12000	0.5	128 (7)	0.24 ± 0.05
		1.0	130 (5)	0.94 ± 0.14
		1.5	130 (5)	1.82 ± 0.21
		2.0	131 (4)	3.03 ± 0.32
	2-7000	0.5	89 (2)	0.46 ± 0.09
		1.0	89 (2)	1.36 ± 0.20
		1.5	88 (3)	2.52 ± 0.31
		2.0	89 (2)	4.11 ± 0.46
	7-12000	0.5	44 (0)	0.11 ± 0.05
		1.0	43 (1)	0.23 ± 0.09
		1.5	42 (2)	0.52 ± 0.14
		2.0	42 (2)	1.11 ± 0.22
APM LSB	2-12000	0.5	176 (10)	0.19 ± 0.04
		1.0	180 (G)	0.78 ± 0.10
		1.5	180 (G)	1.50 ± 0.16
		2.0	180 (6)	2.23 ± 0.22
	2-7000	0.5	83 (G)	0.43 ± 0.08
		1.0	85 (4)	1.41 ± 0.20
		1.5	84 (5)	2.44 ± 0.28
		2.0	85 (4)	3.84 ± 0.44
	7-12000	0.5	97 (0)	0.10 ± 0.04
		1.0	92 (5)	0.18 ± 0.05
		1.5	92 (5)	0.51 ± 0.09
		2.0	93 (4)	0.82 ± 0.13

Table 2. Difference in Mean Counts

Sample	Vel.	Range	POSS	POSS	POSS	1'0SS	APM	APM	APM	APM
		km/s	0.5	1.0	1.5	2.0	0.5	1.0	1.5	2.0
HSB ALL		2-12000	9.6	6.6	6.2	4.9	13.8	9.4	9.9	10.2
		2-7000	4.0	4.0	3.9	3.0	4.8	3.7	4.5	3.7
		7-12000	7.4	7.6	7.5	5.6	8.1	10.4	9.6	8.9
HSB POSS		2-12000	10.5	7.1	6.8	5.8				
		2-7000	5.9	4.3	4.0	3.1				
		7-12000	6.9	7.2	8.0	7.1				
HSB APM		2-12000					2.6	4.3	3.6	3.7
		2-7000					1.7	1.5	1.9	1.1
		7-12000					0.5	3.2	2.1	1.5

Table 3. Nearest Neighbor Summary

Sample	No. Gal.	Vel. Range	Mean Dist.	POSS ks	APM ks
		km/s	Mpc		
HSB ALL	2179	2-12000	0.63 ± 0.01	.23(99)	.23(99)
	1666	2-7000	0.61 ± 0.01	.21(99)	.23(99)
	513	7-12000	0.70 ± 0.02	.34(99)	.32(99)
POSS HSB	747	2-12000	0.574 ± 0.02	.29(99)	
	505	2-7000	0.52 ± 0.02	.29(99)	
	242	7-12000	0.60 ± 0.04	.36(99)	
APM HSB	111	2-12000	0.68 ± 0.05		.19(95)
	91	2-7000	0.66 ± 0.05		.17(85)
	20	7-12000	0.703 ± 0.07		.36(95)
POSS LSB	100	2-12000	0.99 ± 0.06		
	75	2-7000	0.90 ± 0.07		
	25	7-12000	1.25 ± 0.12		
APM LSB	120	2-12000	0.91 ± 0.05		
	76	2-7000	0.79 ± 0.06		
	44	7-12000	1.10 ± 0.08		

Table 4. The Most Isolated LSB Galaxies

Name	Sample	$\alpha(1950)$	$\delta(1950)$	velocity	comments
F834-2	APM	03:36:19.7	+02:12:54	3151	isolated
F834-23	APM	03:49:42.0	-01:39:23	4976	isolated
F851-6	APM	09:11:27.9	-01:39:10	6366	nearby gal.; v=25,000
F851-9	APM	09:18:03.9	-00:28:01	3507	isolated
F851-14	APM	09:27:05.7	+02:25:29	6441	small gal. nearby
F854-2	APM	10:29:51.8	+02:48:45	6592	no chart
F855-28	APM	10:35:35.8	-02:22:49	6249	isolated
F867-19	APM	14:38:30.2	+00:49:56	2734	isolated
F892-10	APM	22:54:58.2	-02:45:24	4605	small gal. nearby
F893-19	APM	23:11:59.4	-00:02:08	4369	isolated
F893-11	APM	23:22:28.2	-00:16:31	5256	interacting
F893-5	APM	23:27:52.0	-00:07:08	5210	small gal. nearby
F894-20	APM	23:32:40.0	-00:14:03	5288	small gal. nearby
F894-2	APM	23:34:47.4	+01:39:21	5263	isolated
F894-1	APM	23:49:17.0	+02:48:13	5323	isolated
F682-1	Poss	00:54:55.2	+10:05:36	2756	isolated
F683-V2	Poss	01:19:28.2	+09:09:36	5680	N509 group ≈ 2.5 Mpc away
F544-V1	Poss	02:09:42.6	+18:15:06	5313	isolated
F704-1	Poss	08:20:47.4	+10:12:36	4237	isolated
F704-V1	Poss	08:22:09.6	+09:23:12	6016	isolated
F638-1	Poss	10:15:42.0	+13:31:48	5471	2 small gal. within .2 Mpc
F568-1	Poss	10:23:22.8	+22:41:00	6526	small gal. .2 Mpc away
F568-3	Poss	10:24:15.0	+22:28:54	5908	isolated
F568-5	Poss	10:27:51.0	+22:06:42	6583	isolated
F638-4	Poss	10:32:04.8	+16:29:24	5856	isolated
F570-5	Poss	11:22:40.8	+18:04:54	4921	isolated
F574-3	Poss	12:25:38.4	+20:27:12	6777	small gal. .2 Mpc away
F574-1	Poss	12:35:37.8	+22:35:18	6890	isolated
F579-V1	Poss	14:30:31.8	+22:59:00	6302	isolated
F511-V1	Poss	14:30:33.6	+22:59:06	6294	isolated
F651-1	Poss	14:35:12.0	+13:31:54	6576	isolated
F740-1	Poss	20:17:22.8	+09:28:36	5493	isolated
F743-1	Poss	21:16:18.0	+08:09:12	2959	isolated
F744-1	Poss	21:45:11.4	+11:57:12	4663	isolated
F745-V1	Poss	21:54:49.8	+08:05:24	3484	isolated
F674-V1	Poss	22:09: 5.4	+15:29:06	6047	isolated
F674-1	Poss	22:16:43.2	+14:46:54	6874	isolated
F750-5	Poss	23:43:01.8	+11:18:06	5367	isolated

Table 5. The Mesh Popular LSB Galaxies

Name	Sample	α (1950)	δ (1950)	velocity	Major Gal.	comments
P824-10	APM	00:25:13.1	+02:21:47	4068	NGC 128	
F824-9b	APM	00:25:43.8	+03:06:26	4036	NGC 128	
F824-9a	APM	00:25:43.8	+03:06:26	3856	NGC 128	
F826-31	APM	01:08:17.1	-00:04:03	5297	NGC 430	A1 94 Supercluster
F827-2	APM	01:14:01.8	+00:56:20	5091	NGC 430	A194
F827-5	APM	01:17:24.7	+00:27:36	4394	IC 1694	A194
F828-1	APM	01:27:54.1	+02:34:28	2115	NGC 520	
F828-9	APM	01:42:29.8	+02:03:46	5403		A194
F831-4	APM	02:29:09.4	+00:04:22	6334	NGC 926	A400 Supercluster
F831-3	APM	02:30:05.1	+00:23:51	6205	IC 232	A400
F831-6	APM	02:32:24.1	+01:02:28	6927	NGC 993	A400
F831-8	APM	02:37:42.1	+02:12:45	6515	NGC 1004	A400
F855-24	APM	10:35:51.6	+00:14:31	5741	NGC 3325	
J<859-8	APM	12:05:30.2	+00:58:33	5882	NGC 4073	Coma Supercluster?
F860-13	APM	12:24:30.7	-00:37:50	2228	NGC 4454	Dwarf in Virgo Supercluster
F863-2	APM	13:50:10.8	+00:22:34	3623	NGC 5184	
F894-5	APM	23:41:48.3	-00:10:52	6636	NGC 7746	
F539-2	1'Oss	0:20:39.0	19:59:36	5716	IC 1543	Persues-Pisces
17473-1	Poss	0:23:20.4	23:38:36	5632	NGC 91	Perseus-Pisces
14611-1	Poss	1:17:7.2	16:31:42	2166	NGC 473	Dwarf Companion to NGC 473?
F612-1	1'Oss	1:27:33.0	14:25:30	2448	NGC 473	
14477-1	POSS	1:51:46.8	22:57:30	4779	NGC 776	Perseus-Pisces
F477-V2	1'Oss	1:51:43.8	22:37:30	5039	NGC 776	Perseus-Pisces
1544-1	Poss	1:58:35.4	19:44:42	2336	NGC 772	Perseus-Pisces
F687-1	1'Oss	2:37:42.6	10:43:54	3662	NGC 1024	
F561-2	1'Oss	8:12:27.0	21:42:42	4276	NGC 2512	Cancer
F495-1	1'Oss	8:13:46.2	23:31:30	4269	NGC 2554	Cancer
F495-2	1'Oss	8:26:5.4	27:2:6	2162	NGC 2592	Cancer Foreground Group
F495-V1	1'Oss	8:25:17.4	25:57:24	2269	NGC 2592	Cancer Foreground Group
14638-3	POSS	10:29:50.4	14:54:24	3160	NGC 3300	
14573-3	1'OSS	12:7:8.4	20:19:36	2494	NGC 4158	Virgo Supercluster
F721-V4	1'Oss	14:0:16.8	10:13:54	5811	NGC 5416	ZW74-23
F650-V1	POSS	14:12:58.2	14:28:54	5249	NGC 5525	Bound to NGC 5525?
F583-1	1'Oss	15:55:16.8	20:48:24	2264	NGC 6035	Hercules Foreground Group
F677-V1	POSS	23:10:19.2	13:47:36	4705	NGC 7535	Pegasus
F677-V4	POSS	23:22:46.2	12:26:30	3664	NGC 7671	Pegasus
F677-V6	POSS	23:25:4.2	13:27:18	3882	NGC 7671	Pegasus

FIGURE CAPTIONS

Figure 1: Top panel: Spatial distribution of POSS LSB galaxies with measured redshifts. Bottom panel: The distribution of redshifts.

Figure 2: Top panel: Spatial distribution of APM LSB galaxies with measured redshifts. Bottom panel: The distribution of redshifts.

Figure 3: Distribution of surface magnitudes for all spirals in *ZCAT* with measured redshift between 2,000 and 12,000 km s⁻¹.

Figure 4: Mean number of cumulative companions at 4 radius bins. In each radius bin the points are offset by 0.1 in the X-axis in order to prevent stacking of symbols. Plotted error bars are $\pm 2\sigma$ in length.

Figure 5: Cumulative distribution functions for the projected distance to the nearest companion galaxy for the 3 HSB and 2 LSB samples.

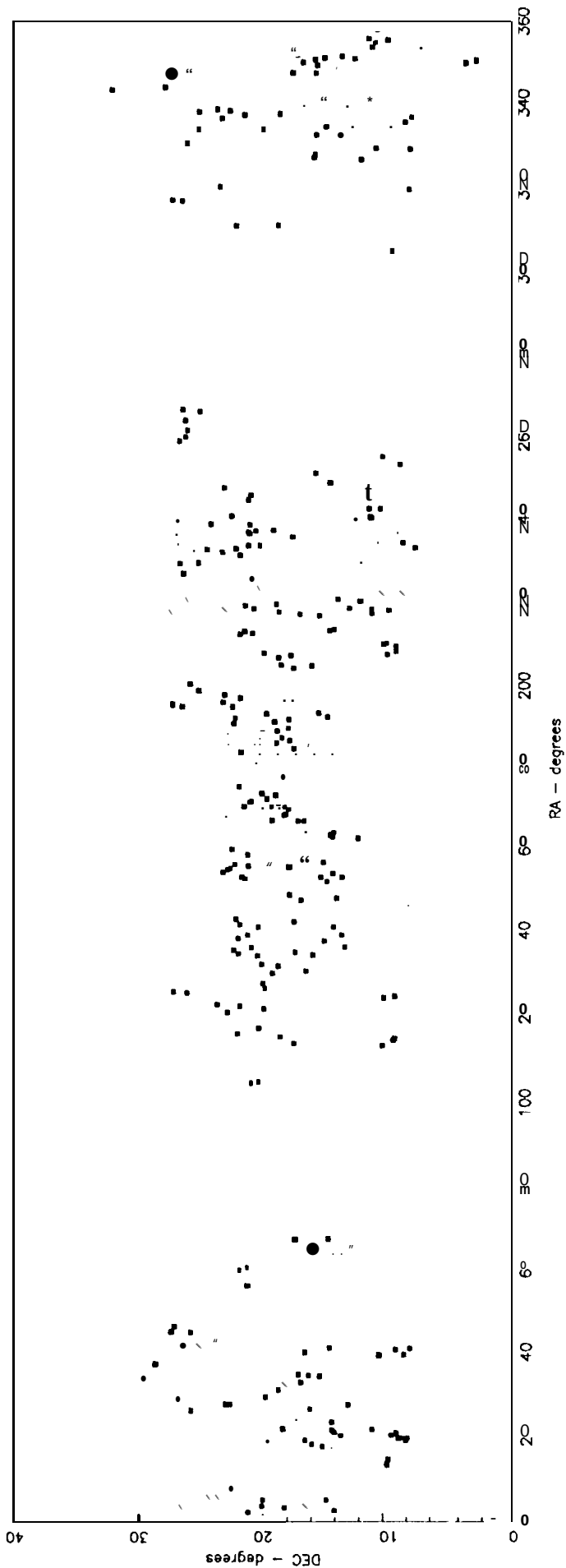
Figure 6: Surface density of galaxies as a function of radius bin. In each radius bin the points are offset by 0.1 in the X-axis in order to prevent stacking of symbols. Plotted error bars are $\pm 2\sigma$ in length.

Figure 7: Histogram showing the number of galaxies with the indicated number of companions inside projected radii of 0.5 and 2.0 Mpc.

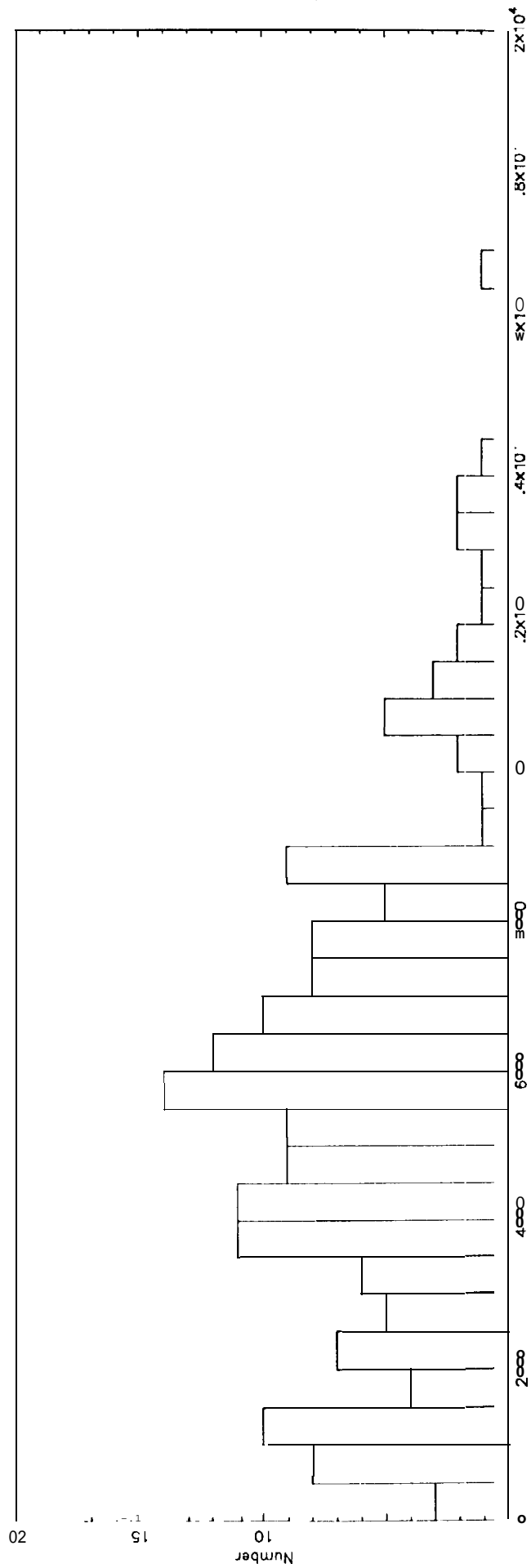
Figure 8: Spatial distribution of isolated and populous LSB galaxies. Open symbols represent isolated galaxies while (Table 4) closed symbols represent populous LSBS (Table 5).

Figure 9: Spatial distribution of other galaxies around the populous galaxies listed in Table 5. The two circles have radii of 1.0 and 2.0 Mpc.

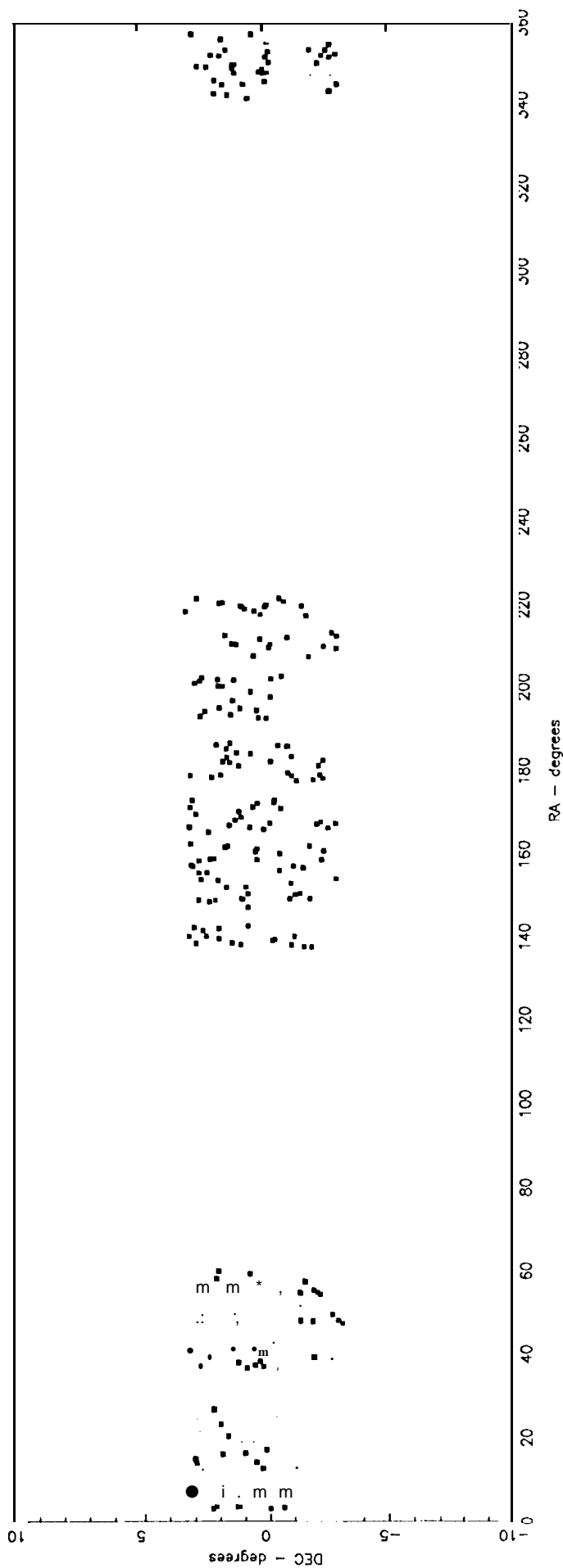
POSS-II



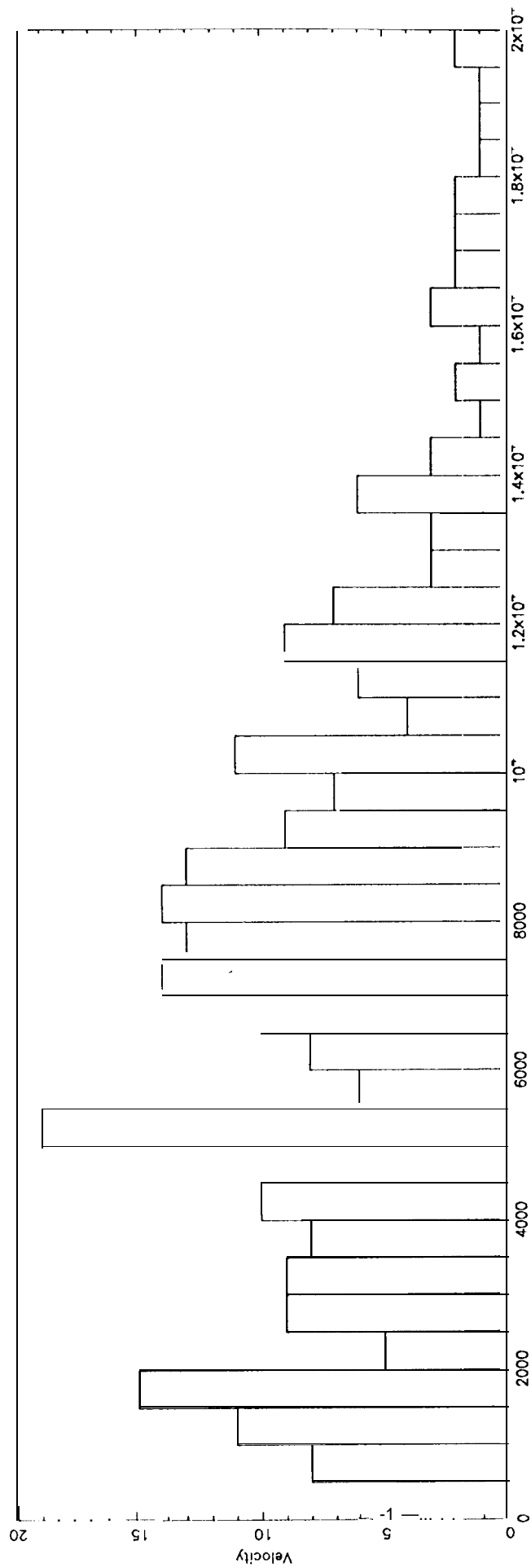
POSS-II LSB



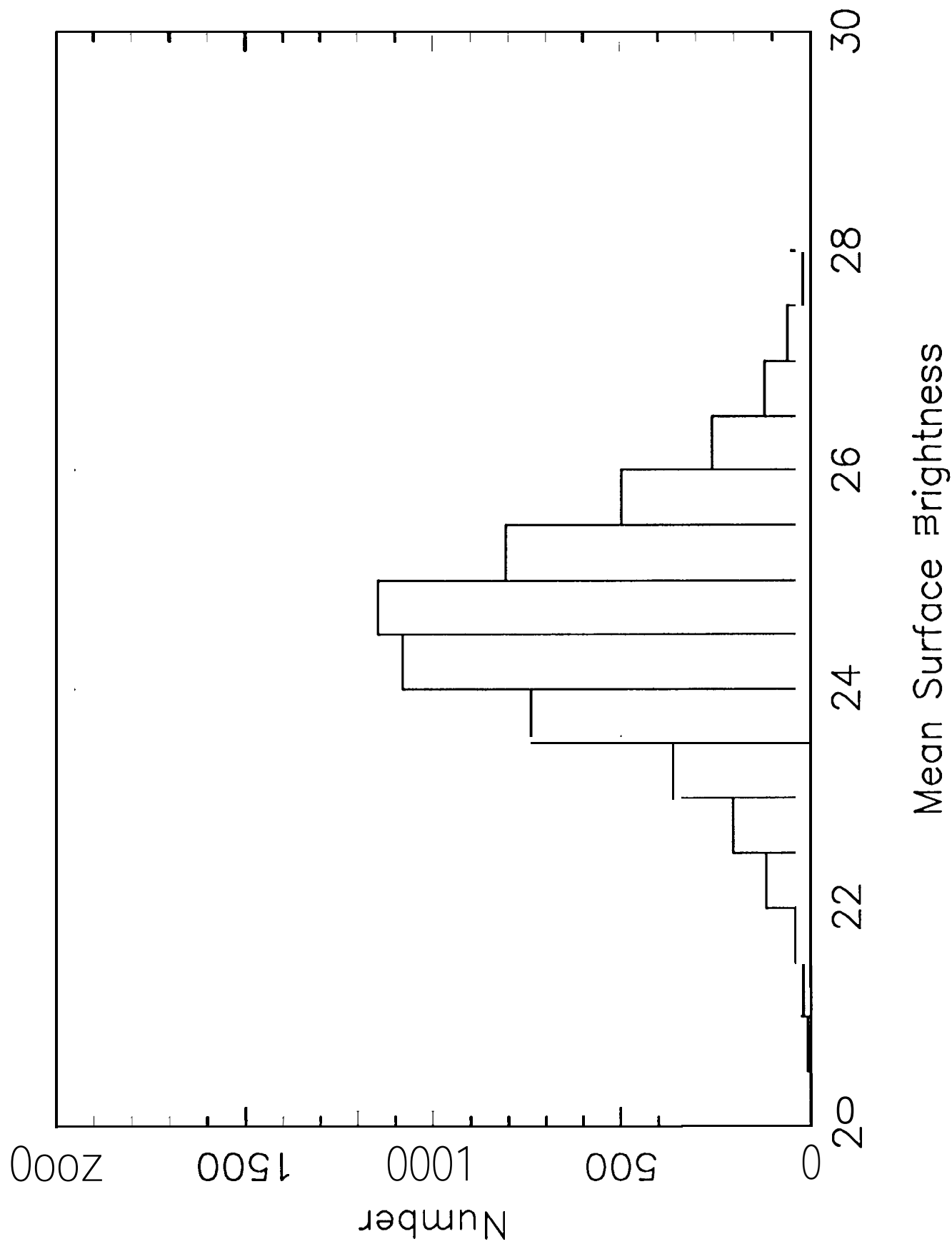
APM



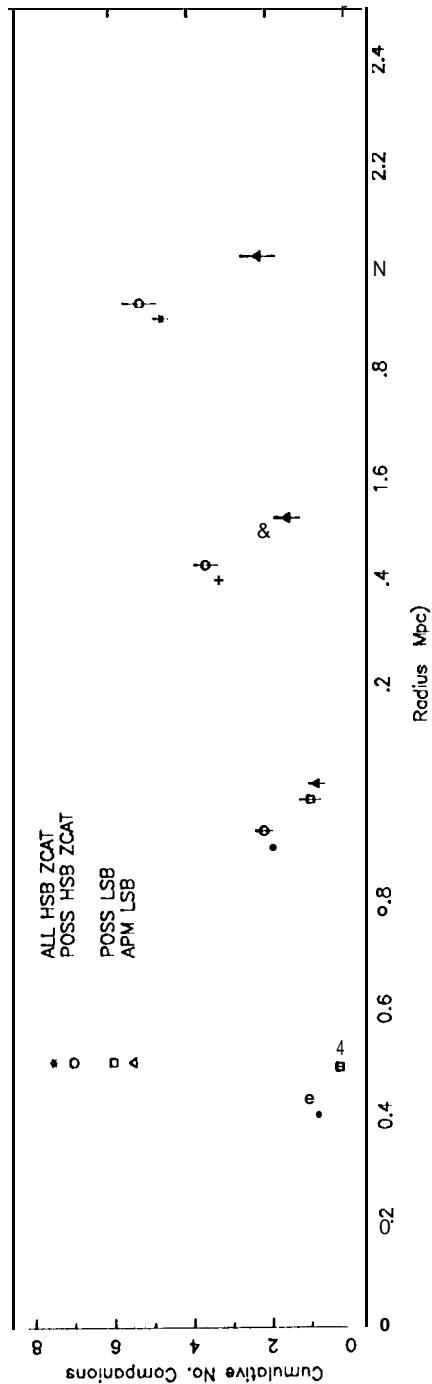
APM LSB



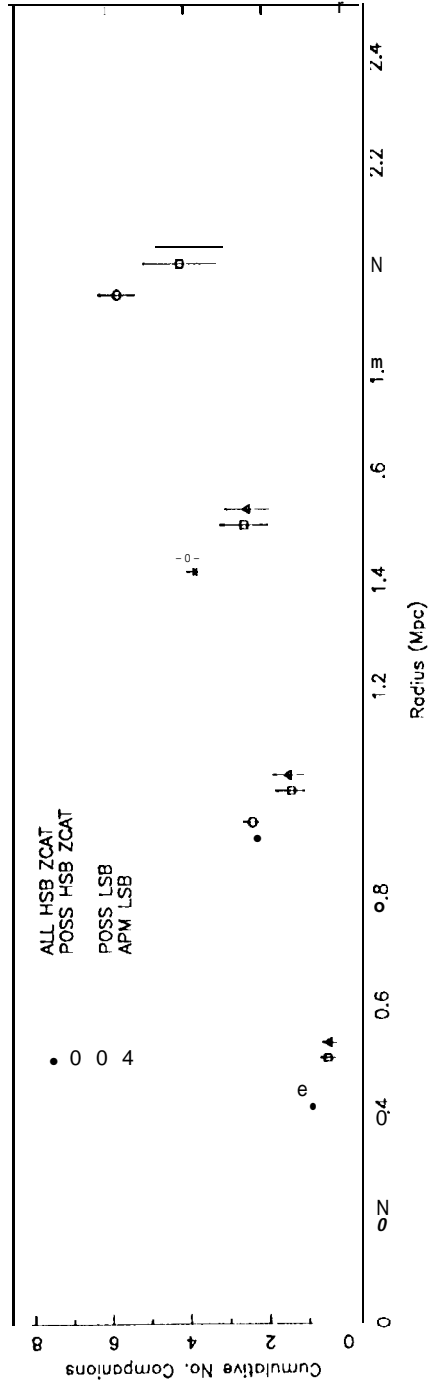
ZCAT Spirals with $2000 < V < 1$



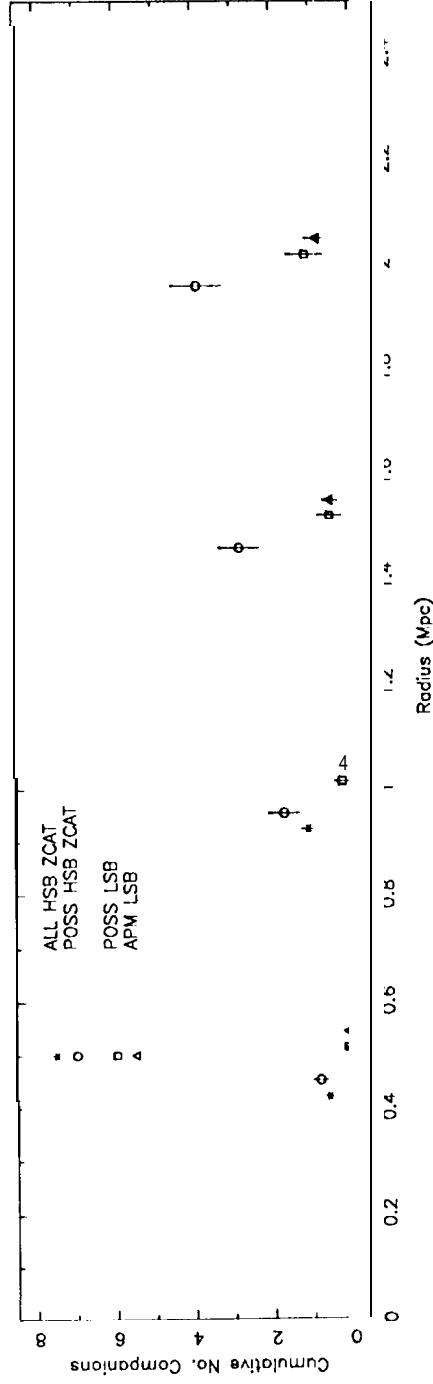
2000 < V < 12000

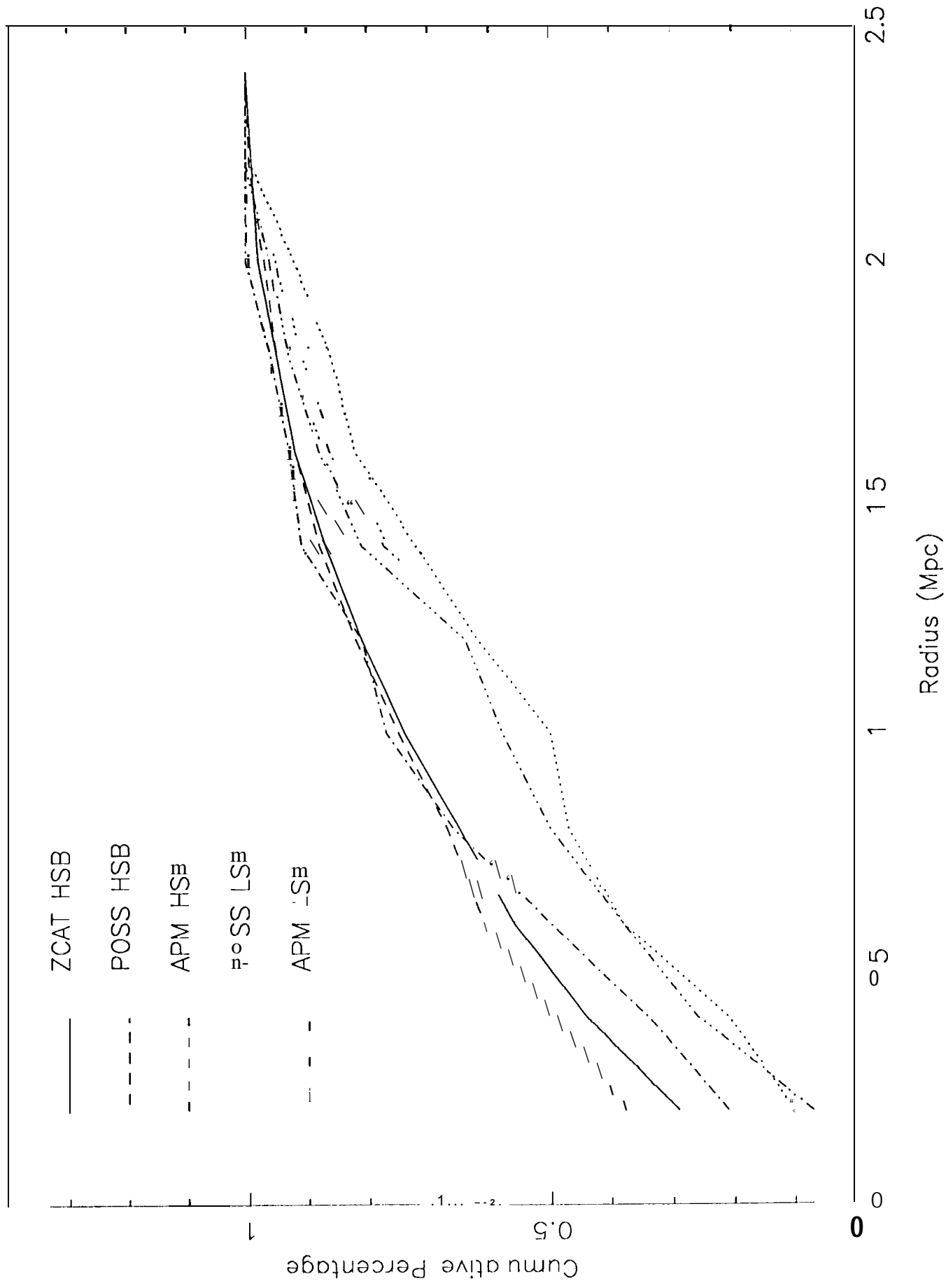


2000 < V < 7000

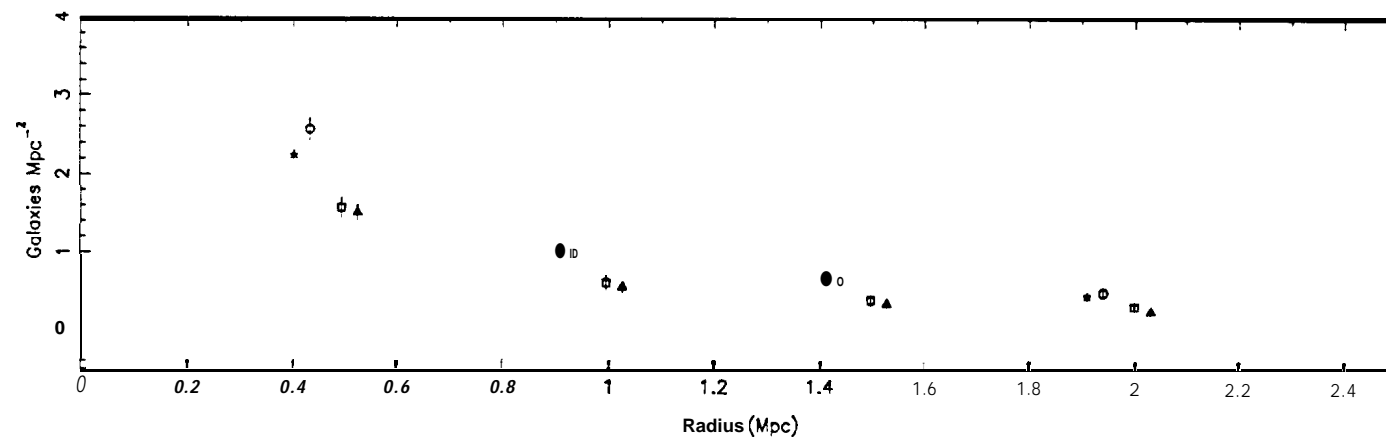


7000 < V < 20000

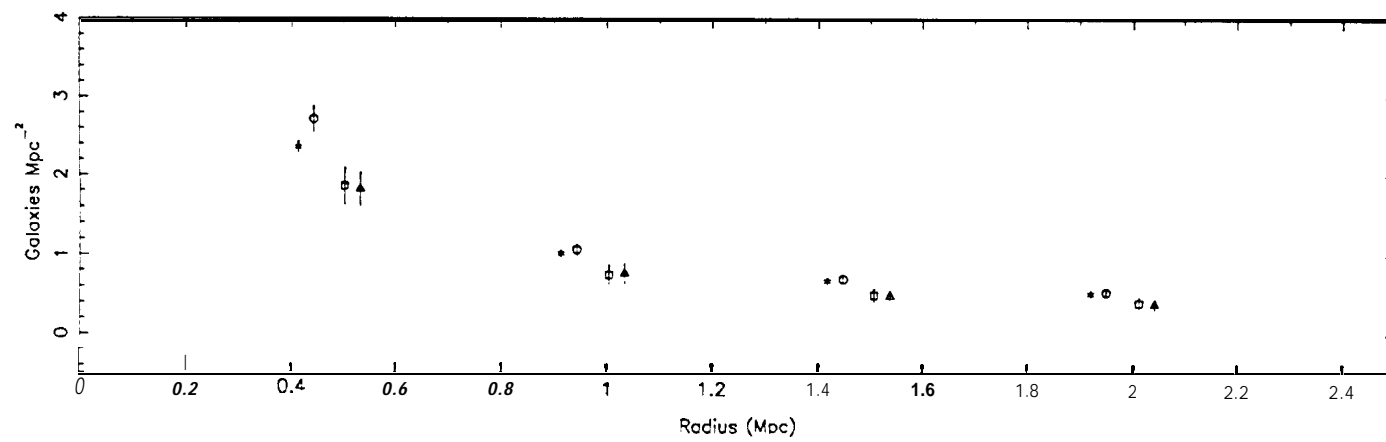




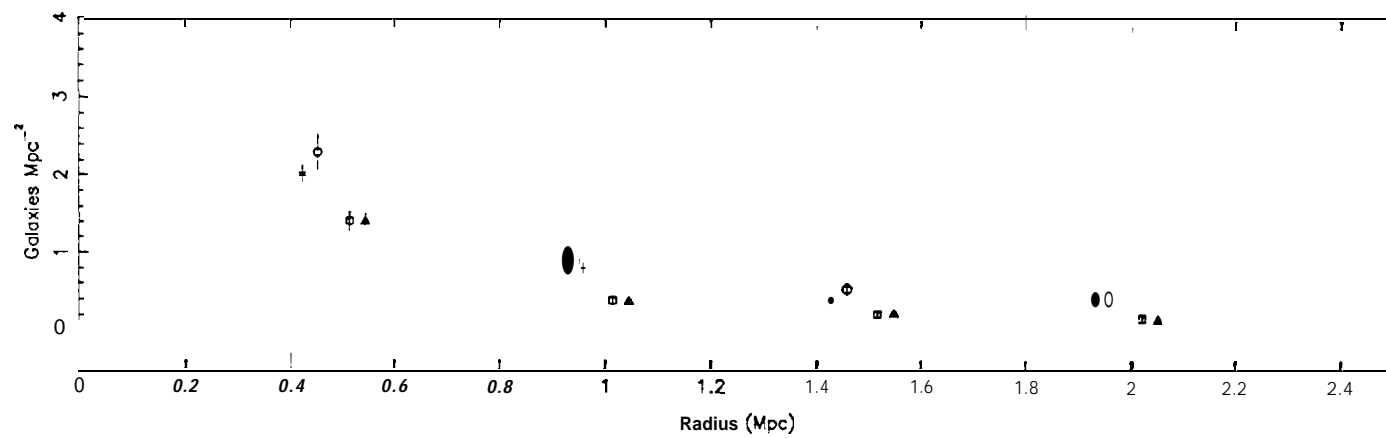
2000 < ν < 12000



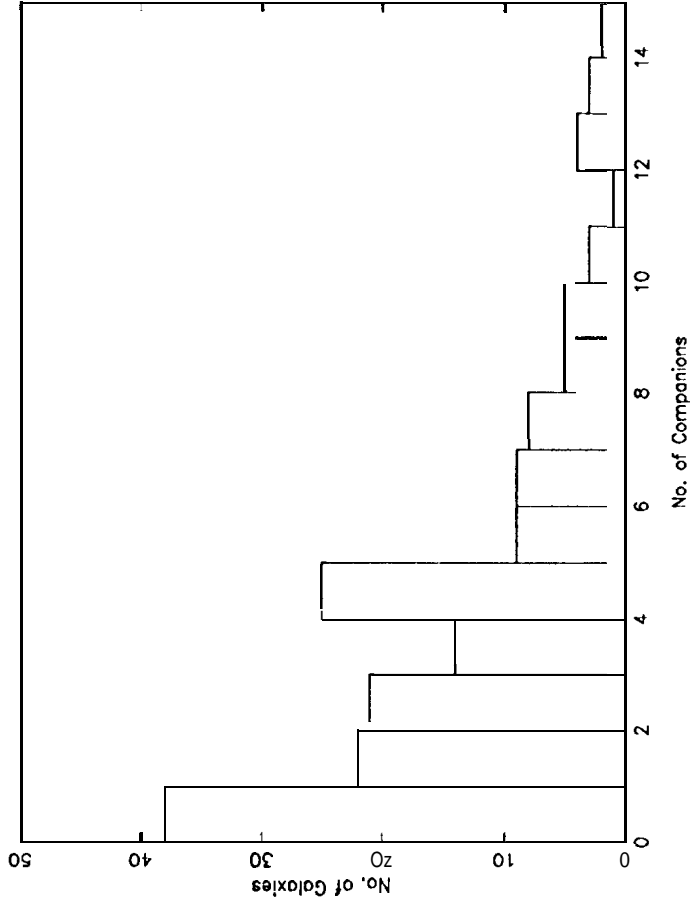
2000 < ν < 7000



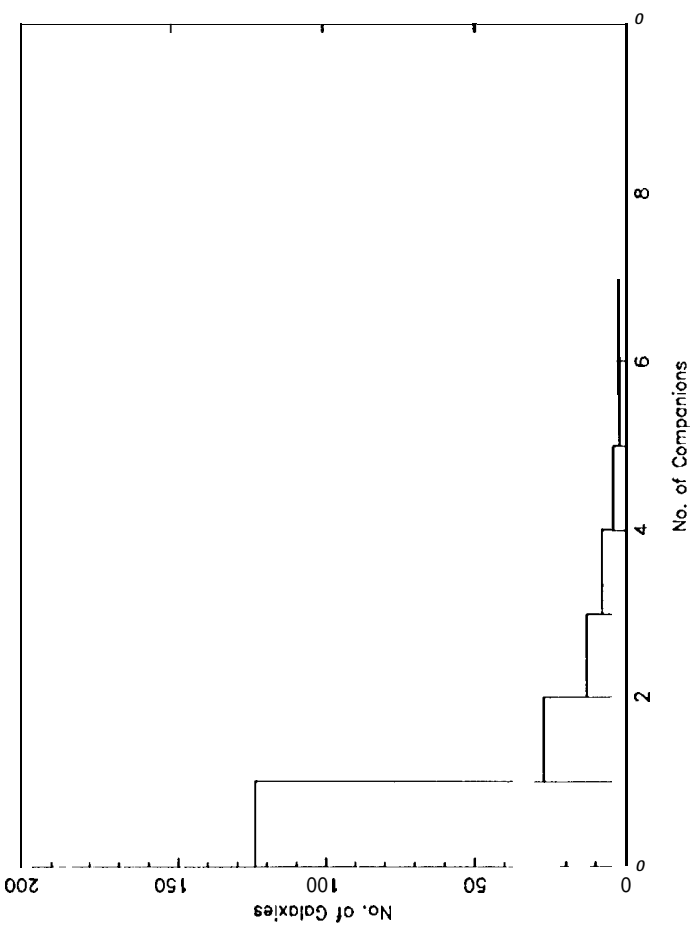
7000 < ν < 12000



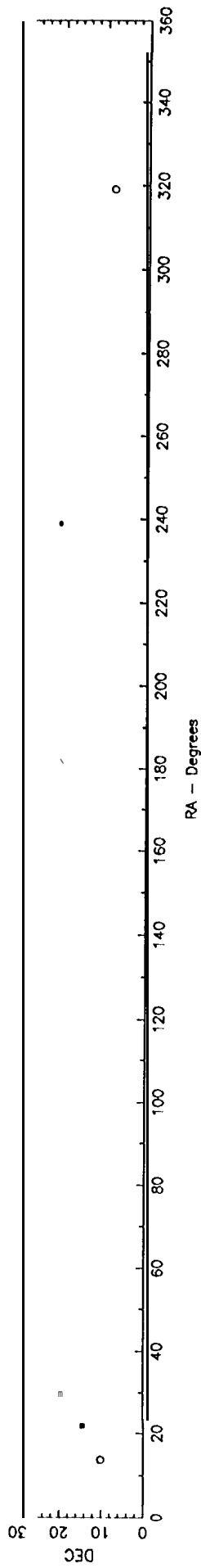
$R < 2$ Mpc



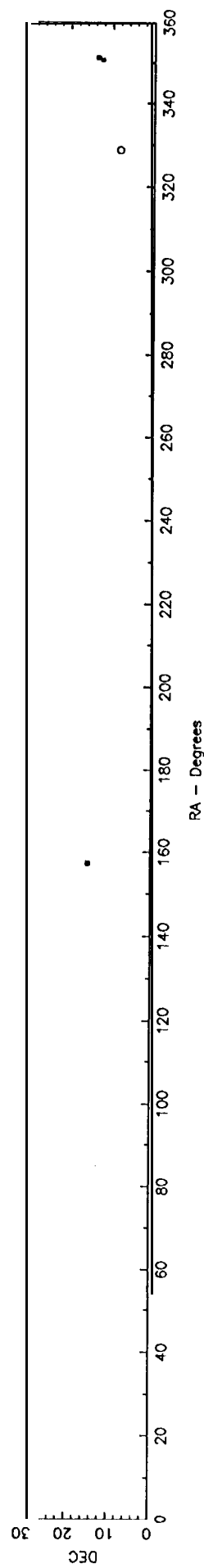
$R < 0.5$ Mpc



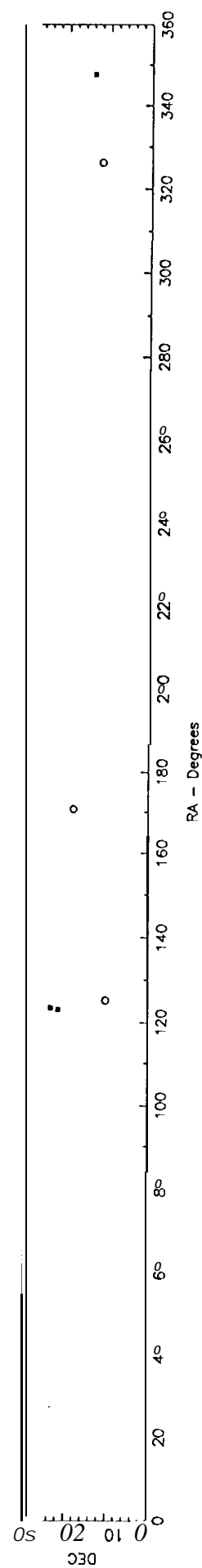
2000 < V < 3000



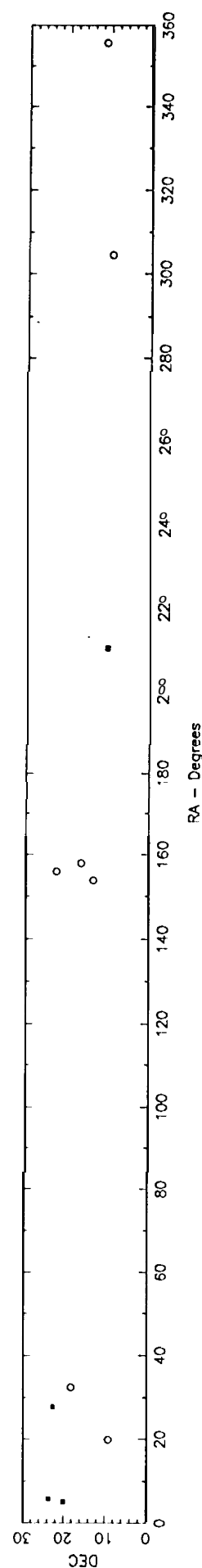
3000 < V < 4000



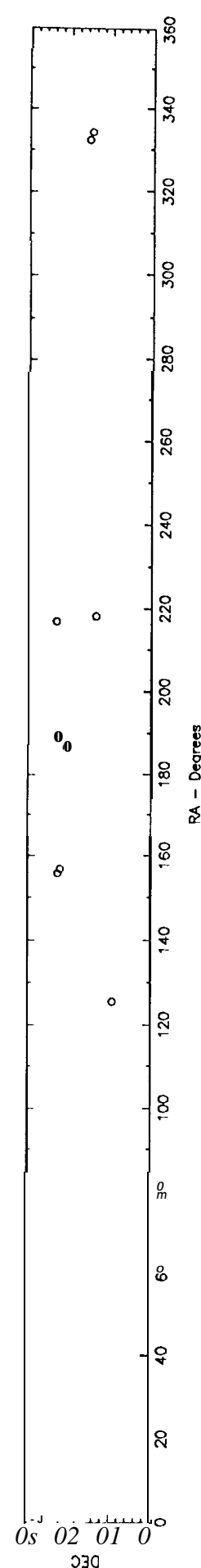
4000 < V < 5000



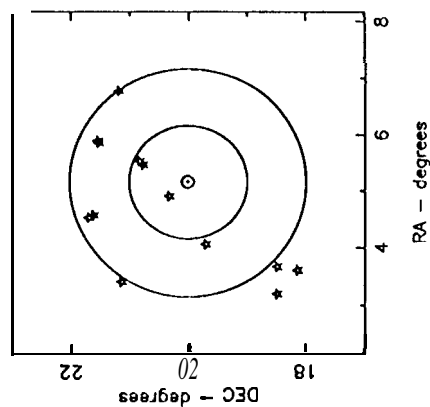
5000 < V < 6000



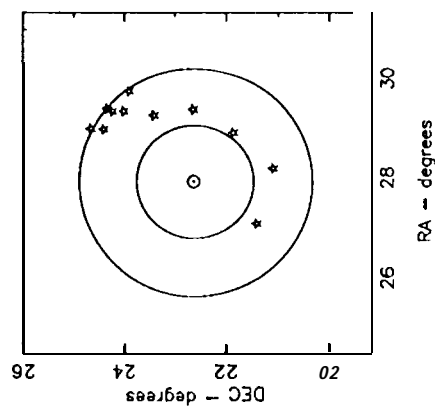
6000 < V < 7000



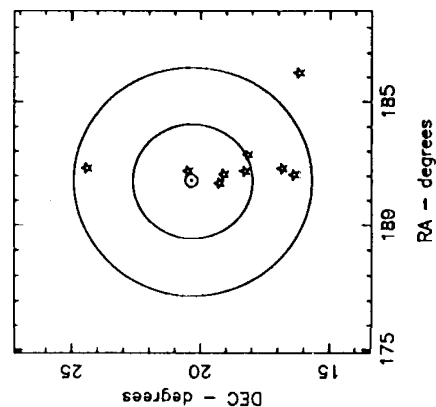
F539-2



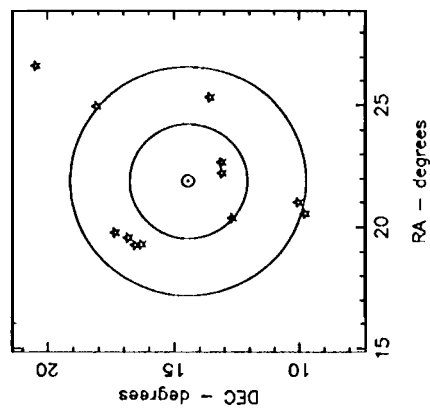
F477-V2



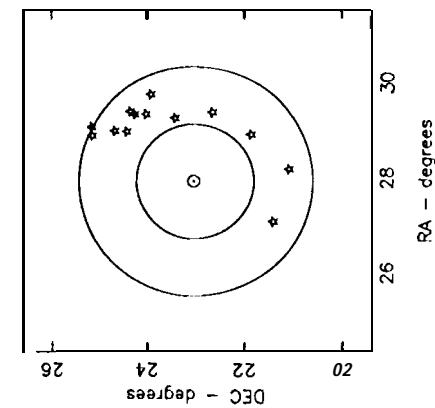
F573-3



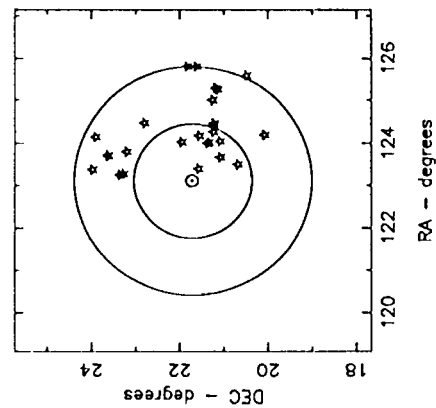
F612-1



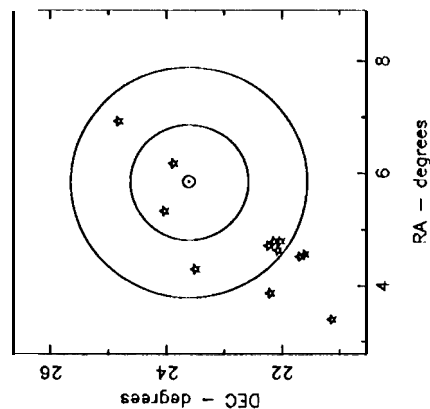
F477-1



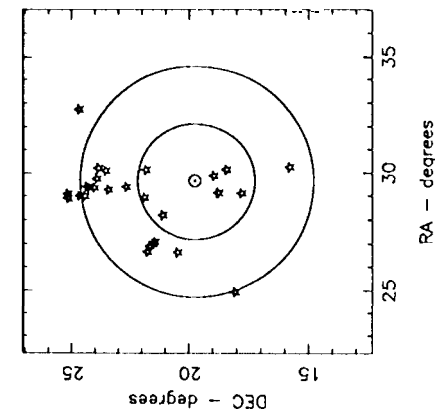
F561-2



F473-1



F544-1



F495-1

